Magnetic field induced confinement-deconfinement transition in graphene quantum dots

G. Giavaras, P. A. Maksym, and M. Roy
Department of Physics and Astronomy, University of Leicester, Leicester LE1 7RH, UK
(Dated: May 21, 2008)

Massless Dirac particles cannot be confined by an electrostatic potential. This is a problem for making graphene quantum dots but confinement can be achieved with a magnetic field and here, general conditions for confined and deconfined states are derived. There is a class of potentials for which the character of the state can be controlled at will. Then a confinement-deconfinement transition occurs which allows the Klein paradox to be probed experimentally in graphene dots.

PACS numbers: 73.21.La, 73.63.Kv, 73.63.-b, 81.05.Uw

Single layer graphene is attracting attention because its charge carriers are massless, relativistic particles [1]. The relativistic effects result from a unique, zero-gap band structure that leads to quantum states described by the two-component Dirac-Weyl equation. This allows relativistic physics to be explored in a solid state system and has many potential applications ranging from high frequency electronics [1] to quantum computing [2]. In particular, graphene quantum dots are very attractive as spin qubits because they are expected to have low spin decoherence [2]. However there is a problem with making graphene dots for quantum computing or any other application: relativistic effects prevent massless particles from being confined by an external potential.

The problem results from the Klein paradox [3, 4, 5]. When relativistic particles with mass are incident on a 1D potential barrier, the state in the barrier decays exponentially unless the barrier height exceeds the threshold for pair production, at which point the state in the barrier becomes oscillatory. The paradox is that any attempt to enhance the localisation by increasing the barrier height eventually destroys it. But there is no threshold for pair production for massless particles so exponential decay and bound states do not occur.

Graphene dots can be formed from external potentials or nanocrystals. The quantum states [6, 7, 8, 9], in external potentials [10] are quasi-bound: they have a low amplitude oscillatory tail and are similar to the scattering resonances studied in undergraduate physics. A perpendicular magnetic field enhances the localisation of these states [7] and true bound states can occur in graphene dots defined by a spatially non-uniform field [8]. So a magnetic vector potential has a localising effect that tends to cancel the delocalising effect of a scalar potential. But what are the general conditions for confined states to occur when an electrostatic scalar potential and a magnetic vector potential are applied to graphene simultaneously?

This question is answered in the present Letter. It is shown that both true bound states and quasi-bound states occur, depending on the form of the potentials. In addition, there is a third and most interesting possibility. In some cases, the character of the states depends on the parameters of the potentials and can be controlled at will. A confinement-deconfinement transition then occurs in which the character of the states changes from oscillatory to exponential as in the Klein paradox for particles with mass. This gives a way of probing the Klein paradox experimentally in a solid state system and numerical studies of the quantum states in a realistic dot model show it is feasible.

The system considered here is a cylindrically symmetric graphene dot. The dot region is defined by an electrostatic potential, $V(r)$, and the magnetic vector potential, $A_\theta(r)$, is in the azimuthal (θ) direction. The functional form of these potentials has a significant effect on the character of the states. In particular, when V and A_θ increase as power laws, $V = V_0 r^s$, $A_\theta = A_0 r^t$, $s, t > 0$, the character of the states depends critically on s and t. If $s > t$ the states oscillate in the asymptotic regime of large r but decay exponentially when $s < t$. In both cases the asymptotic character of the states is independent of V_0 and A_0 but when $s = t$ the character of the states does depend on these constants and a transition from exponential to oscillatory behaviour occurs when V_0 is increased or A_0 is decreased. This is the confinement-deconfinement transition.

The two-component envelope function, ψ, satisfies $(V + \gamma\boldsymbol{\sigma}\cdot\boldsymbol{\pi}/\hbar)\psi = E\psi$, where $\boldsymbol{\sigma}$ are the Pauli matrices, $\boldsymbol{\pi} = \mathbf{p} + e\mathbf{A}$ and $\gamma = 646$ meV nm [7]. For cylindrically symmetric systems $\psi = (\chi_1(r)\exp(i(m-1)\theta), \chi_2(r)\exp(im\theta))$ where m is the angular momentum quantum number. The radial functions χ_1 and χ_2 satisfy

$$\frac{V}{\gamma}\chi_1 - i\frac{d\chi_2}{dr} - i\frac{m}{r}\chi_2 - i\frac{e}{\hbar}A_\theta\chi_2 = \frac{E}{\gamma}\chi_1, \quad (1)$$

$$-i\frac{d\chi_1}{dr} + i\frac{(m-1)}{r}\chi_1 + i\frac{e}{\hbar}A_\theta\chi_1 + \frac{V}{\gamma}\chi_2 = \frac{E}{\gamma}\chi_2. \quad (2)$$

These equations can be uncoupled by differentiating them and this leads to the relation

$$\chi_2'' + a(r)\chi_2' + b(r)\chi_2 = 0, \quad (3)$$

where

$$a(r) = \frac{1}{r} + \frac{1}{E-V}\frac{dV}{dr}, \quad (4)$$

$$b(r) = -\frac{m^2}{r^2} + \left(\frac{m}{r} + \frac{e}{\hbar}A_\theta\right)\frac{1}{E-V}\frac{dV}{dr} - \frac{(2m-1)}{r}\frac{e}{\hbar}A_\theta + \frac{e}{\hbar}\frac{dA_\theta}{dr} + \frac{(E-V)^2}{\gamma^2} - \frac{e^2}{\hbar^2}A_\theta^2. \quad (5)$$

The first order derivative in Eq. (3) is eliminated by putting $\chi_2(r) = u_2(r)\exp(-\int a(r)dr/2)$ which gives

$$u_2'' + k_2^2(r)u_2 = 0, \quad (6)$$

where $k_2^2(r) = b - a'/2 - a^2/4$. Although k_2^2 diverges when $E = V$, χ_2 is regular there. Since $\exp(-\int a(r)dr/2)$ is not an oscillatory function of r, u_2 has the same character as χ_2. Eq. (6) shows that this character is oscillatory when k_2^2 is positive and exponential when k_2^2 is negative. Asymptotic exponential decay is characteristic of a bound state but here "confined" is used to indicate a bound state that is localised near the centre of the dot.

When V and A_θ increase as power laws, the asymptotic form of k_2^2 is $(V_0/\gamma)^2 r^{2s} - (eA_0/\hbar)^2 r^{2t}$. Hence k_2^2 is positive when $s > t$, leading to oscillatory character and deconfined states. And k_2^2 is negative when $s < t$, leading to exponential character and confined states. However if $s = t$ the asymptotic form is $[(V_0/\gamma)^2 - (eA_0/\hbar)^2]r^{2t}$ so the sign of k_2^2 depends on V_0 and A_0 and a confinement-deconfinement transition occurs when $V_0^2 = (\gamma e A_0/\hbar)^2$. This also follows from the uncoupled equation for χ_1: the corresponding k^2-value, $k_1^2 \neq k_2^2$ but $k_1^2 \to k_2^2$ in the asymptotic limit so χ_1 and χ_2 have the same character.

To investigate the states further, Eqs. (1) and (2) are solved numerically. The Hamiltonian, H, satisfies

$$\int_0^R \int_0^{2\pi} [\psi_\alpha^* H\psi_\beta - (H\psi_\alpha)^*\psi_\beta]\, d\theta r dr = -2\pi i\gamma\left[(\chi_{1\alpha}^*\chi_{2\beta} + \chi_{2\alpha}^*\chi_{1\beta})r\right]_0^R, \quad (7)$$

where ψ_α and ψ_β are two-component states of angular momentum m and $\chi_{i\alpha}$,$\chi_{i\beta}$ are the corresponding radial functions. Eqs. (1) and (2) lead to a Hermitian eigenvalue problem when the boundary terms in Eq. (7) vanish. For this to happen it is sufficient that one component is regular at the origin and one component vanishes at the boundary, R. Then it follows from Eqs. (1) and (2) that both components are regular at the origin but it does not follow that both components vanish at R. However a true bound state has an exponential tail so both components of a bound state vanish in the limit of large R. Hence confined and deconfined states can be distinguished by solving Eqs. (1) and (2) subject to the boundary conditions that one component is regular at the origin and *one* component vanishes at R and then looking for an exponential tail in *both* components.

Eqs. (1) and (2) are solved by discretizing them on a uniform grid. By applying the time reversal operator to Eqs. (1) and (2) it can be shown that $E(m, A_0) = E(1-m, -A_0)$. It is important to ensure that the eigenvalues of the discretized Hamiltonian have the same property and this requires identical numbers of grid points for χ_1 and χ_2. This excludes the use of centred differences [11] so d/dr is approximated by the forward difference operator L_f or the backward difference operator L_b. The procedure depends on m. When $m \leq 0$, $\chi_2(R)$ is chosen to vanish [12], L_f is used to find $d\chi_2/dr$ and L_b to find $d\chi_1/dr$ and vice-versa when $m \geq 1$. Although this guarantees that $E(m, A_0) = E(1-m, -A_0)$, it has the disadvantage that numerical errors are linear in the step length Δr. To compensate for this, Δr is kept small and all the eigenvalues computed in this work are accurate to about 1 part in 10^3, except for $s = 2, t = 1$ and $s = 2, t = 2$, where there are rapid oscillations but the accuracy is still better than 2%. The discretization leads to a non-Hermitian matrix eigenvalue problem. A similarity transformation is used to reduce this to a real, symmetric eigenvalue problem which is solved numerically.

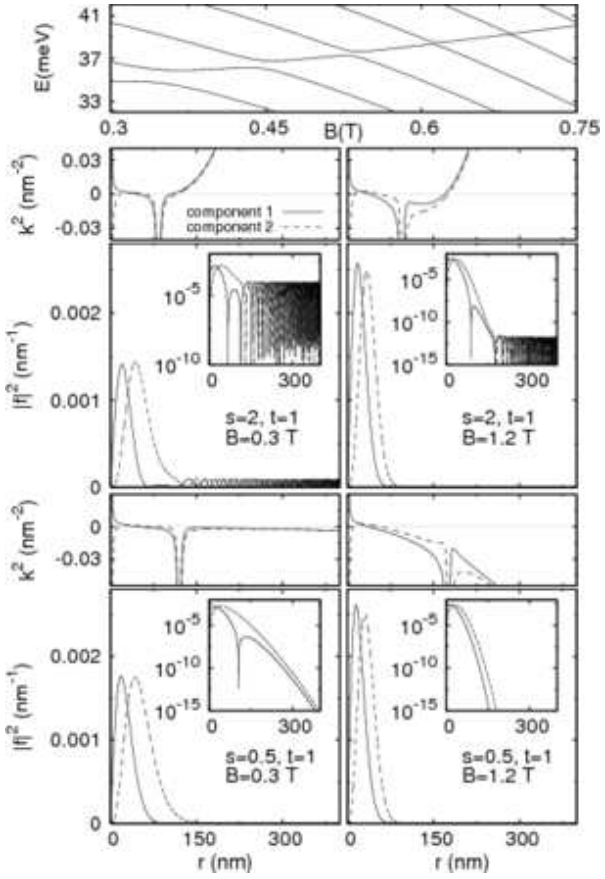

FIG. 1: Confined and deconfined states for cases when no transition occurs. The frame above each state shows k_i^2. Topmost frame: $E(B)$ for $s = 2$, $t = 1$.

The quantum states shown in the present work are all $m = 1$ states. Other states exhibit similar features, although the amplitude of oscillations is m-dependent [7]. Since the main focus of this work is on the confinement-deconfinement transition, the states are selected so that the behaviour at the origin does not change significantly when the potential parameters are changed. All the

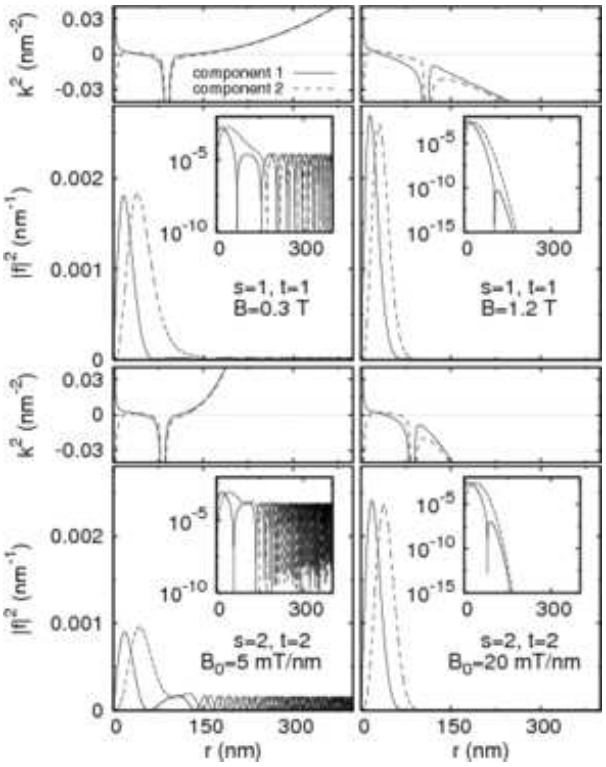

FIG. 2: As Fig. 1 but for two cases which exhibit a confinement-deconfinement transition.

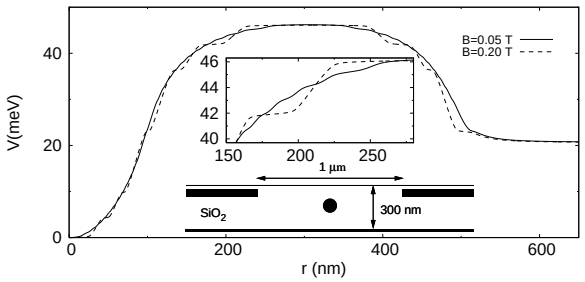

FIG. 3: $V(r)$ for the gate geometry shown in the bottom inset.

states have been selected to have a large amplitude close to the origin and can be regarded as dot states. The energies as a function of magnetic field typically show a series of anti-crossings (Fig. 1) and where necessary, the line of anti-crossings is followed to preserve the qualitative form of the state at the origin [13]. Every energy computed here is between 26 and 67 meV, within the validity limit of the linear graphene Hamiltonian ($\approx \pm 1$ eV [1]).

Confined and deconfined states are illustrated in Fig. 1. The radial probability distribution, $|f_i|^2 \equiv r|\chi_i|^2$, $i = 1, 2$ is shown together with k_i^2. The insets show $|f_i|^2$ on a logarithmic scale. $R = 600$ nm, large enough to ensure that the asymptotic sign of k_i^2 has been reached. The magnetic field, B, is uniform. When $s = 2$, $t = 1$, $V_0 = 5 \times 10^{-3}$ meV nm^{-2}, the asymptotic sign of k_i^2 is positive and the asymptotic character of $|f_i|^2$ is oscillatory independent of B. The amplitude of the oscillations decreases with increasing B. When $s = 0.5$, $t = 1$, $V_0 = 5$ meV nm$^{-1/2}$ and $B \neq 0$, the asymptotic sign of k_i^2 is negative and the asymptotic character of $|f_i|^2$ is exponential, as can be seen from the insets.

The confinement-deconfinement transition is illustrated in Fig. 2. $R = 600$ nm, again large enough to reach the asymptotic regime. When $s = 1$, $t = 1$, $V_0 = 0.5$ meV nm^{-1} and $B = 0.3$ T, the asymptotic sign of k_i^2 is positive and the asymptotic character is oscillatory. In contrast, when $B = 1.2$ T, the asymptotic sign of k_i^2 is negative and the asymptotic character is exponential. The transition also occurs in non-uniform magnetic fields and it may be possible to generate a suitable field by putting a dot under a superconducting obstacle in a uniform field. Fig. 2 (bottom) shows the transition for $s = 2$, $t = 2$, $V_0 = 5 \times 10^{-3}$ meV nm^{-2}, that is parabolic confinement in a linearly increasing field, $B(r) = B_0 r$.

In any real quantum dot, the scalar potential would approach a finite asymptotic value instead of increasing without limit. Consequently, all the states of a graphene dot in a magnetic field have an exponential tail. However, an effect similar to the confinement-deconfinement transition occurs in the middle distance region between the centre of the dot and the asymptotic regime.

For this transition to be observable, the dot level has to be in the region of very low density of states between the bulk Landau levels. This requires a potential similar to the one shown in Fig. 3. The asymptotic value of the potential is engineered to be just below the dot level. This puts the dot level between the zeroth and first Landau levels. Thus the dot level can be isolated from the bulk Landau levels provided that they are narrow enough.

The required potential can be generated by gate electrodes. One possible arrangement is a metal plate with a circular hole that contains an electrode. The graphene sheet is above these electrodes on 300 nm of SiO_2 on a back-gate at 0 V. The plate (-1 V) generates the asymptotically flat part of the potential, the hole generates the barrier and the central electrode (-2 V) generates the well. Similar gated, monolayer graphene nanostructures have been fabricated recently [14]. The potential in Fig. 3 was computed by solving the Poisson equation on a discrete mesh. Screening by the graphene sheet was treated in the Thomas-Fermi approximation [15]. The resulting potential is magnetic field dependent because the density of states is field dependent. This causes steps in the potential (inset to Fig. 3) which occur when the number of occupied Landau levels changes. However the field dependence is weak at the low fields considered here.

The "confinement-deconfinement" transition for the potential in Fig. 3 and a uniform magnetic field is shown in Fig. 4. For all fields, the states have a peak near the centre of the dot and an exponential tail. The transition occurs in the middle distance region between these two features, $200 \lesssim r \lesssim 400$ nm. For any potential, this re-

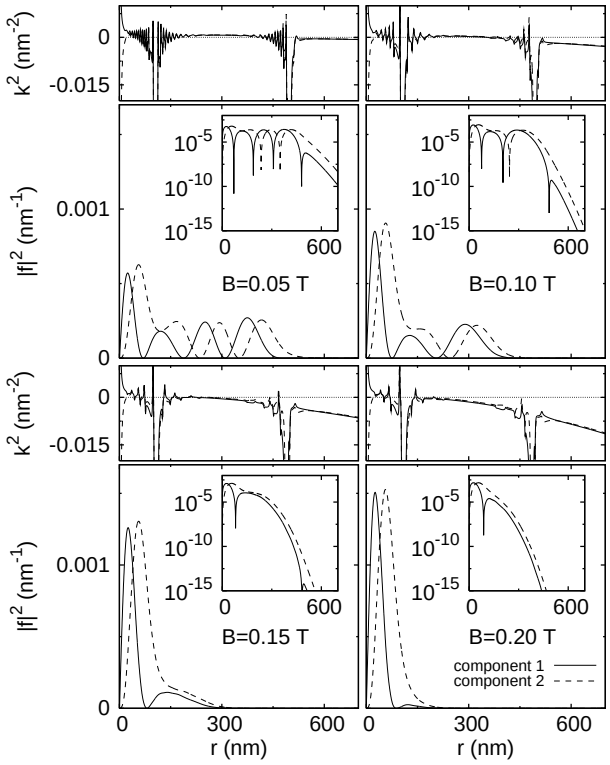

FIG. 4: Confinement-deconfinement transition. As Fig. 2 but for the potential shown in Fig. 3.

gion can be identified by computing k_i^2. In Fig. 4, this varies rapidly because of the steps in the potential but remains positive in the middle distance region when B = 0.05 T. At this field, the oscillations in $|f_i|^2$ correspond to those in Fig. 2 but are much less rapid because V, hence k_i^2 is smaller. As the field increases the region of positive k_i^2 shrinks and a transition to exponential behaviour occurs. This is analogous to the change of character seen in the Klein paradox for relativistic particles with mass.

The occurrence of the transition is insensitive to the electrode geometry. The one in Fig. 3 has the advantage that the graphene is easy to access but may be difficult to fabricate. However, similar transitions occur in systems with disk or spherical central electrodes with the plate and central electrode either above or below the graphene sheet. In addition, calculations for model potentials with a well, barrier and flat portion show that the occurrence of the transition is insensitive to the model parameters. The only requirement is a region where k_i^2 changes sign when A_0 increases. This is relatively easy to arrange.

$|f_i|^2$ in Fig. 4 decreases by 3-4 orders of magnitude at $r \approx 300$ nm when the character of the state changes from oscillatory to exponential. This large effect could be used to probe the transition experimentally. For example, the decrease in $|f_i|^2$ causes a decrease in the local density of states (LDOS) near the dot which could be detected with scanning tunnelling microscopy. The decrease in $|f_i|^2$ would also cause a large decrease in the overlap of the dot state with states in contacts at $r \approx 300$ nm. This could be detected by looking for a change in transport through the dot state via diametrically opposite contacts at $r \approx 300$ nm. Numerical calculations of the LDOS for the potential in Fig. 3 show that the state in Fig. 4 lies in a region of very low bulk density of states, with the dot state around 0.1-0.2 meV away from any other levels. This suggests the dot state can be resolved experimentally in graphene samples of sufficient quality.

In summary, confined and deconfined states occur in graphene dots in a magnetic field. The states are confined when the scalar potential rises slowly and deconfined when it rises rapidly. But when the scalar and vector potentials have the same power law, the character of the states can be controlled at will and a confinement-deconfinement transition occurs. A similar effect occurs in a realistic dot model. This is analogous to the relativistic Klein paradox and may be experimentally observable. The proposed system may be attractive because it allows graphene dots to be formed in a uniform magnetic field.

It is a pleasure to acknowledge useful discussions with Professors H. Aoki, H. Fukuyama and S. Tarucha. This work was supported by the UK Engineering and Physical Sciences Research Council.

[1] A. K. Geim and K. S. Novoselov, Nature Materials **6**, 183 (2007).
[2] B. Trauzettel, D. V. Bulaev, D. Loss and G. Burkard, Nature Physics **3**, 192 (2007).
[3] M. I. Katsnelson, K. S. Novoselov and A. K. Geim, Nature Phys. **2**, 620 (2006).
[4] N. M. R. Peres, A. H. Castro Neto and F. Guinea, Phys. Rev. B **73**, 241403(R) (2006).
[5] Vadim V. Cheianov and Vladimir I. Fal'ko, Phys. Rev. B **74**, 041403(R) (2006).
[6] P. G. Silvestrov and K. B. Efetov, Phys. Rev. Lett. **98**, 016802 (2007).
[7] Hong-Yi Chen, Vadim Apalkov and Tapash Chakraborty, Phys. Rev. Lett. **98**, 186803 (2007).
[8] A. De Martino, L. Dell'Anna and R. Egger, Phys. Rev. Lett. **98**, 066802 (2007).
[9] A. Matulis and F. M. Peeters, arXiv:0711.4446v1 (2007).
[10] The physics of nanocrystals is expected to be different.
[11] Centred differences require different numbers of grid points for χ_1 and χ_2 and lead to unphysical solutions which are not smooth in the limit of zero step size.
[12] The alternative choice, $\chi_1(R) = 0$ is incompatible with the discretization used in the present work.
[13] In many cases the anti-crosssings disappear at a sufficiently high field.
[14] B. Huard, J. A. Sulpizio, N. Stander, K. Todd, B. Yang and D. Goldhaber-Gordon, Phys. Rev. Lett. **98**, 236803 (2007).

[15] D. P. DiVincenzo and E. J. Mele, Phys. Rev. B **29**, 1685 (1984).